



HAL
open science

Effects of polydispersity and high scatterer concentration on quantitative ultrasound estimates

Olivier Lombard, Myléna Audenay, Emilie Franceschini

► To cite this version:

Olivier Lombard, Myléna Audenay, Emilie Franceschini. Effects of polydispersity and high scatterer concentration on quantitative ultrasound estimates. IEEE International Ultrasonics Symposium, Oct 2022, Venice, Italy. pp.1-5. hal-03850666

HAL Id: hal-03850666

<https://hal.science/hal-03850666>

Submitted on 14 Nov 2022

HAL is a multi-disciplinary open access archive for the deposit and dissemination of scientific research documents, whether they are published or not. The documents may come from teaching and research institutions in France or abroad, or from public or private research centers.

L'archive ouverte pluridisciplinaire **HAL**, est destinée au dépôt et à la diffusion de documents scientifiques de niveau recherche, publiés ou non, émanant des établissements d'enseignement et de recherche français ou étrangers, des laboratoires publics ou privés.

Effects of polydispersity and high scatterer concentration on quantitative ultrasound estimates

Olivier Lombard^{1*†}, Mylena Audenay^{*}, Emilie Franceschini^{*}

Email: olivier.lombard@univ-avignon.fr, mylena.audenay@centrale-marseille.fr, franceschini@lma.cnrs-mrs.fr

^{*}Aix-Marseille Univ, CNRS, Centrale Marseille, LMA, Marseille, France

[†]Université d'Avignon, UMR EMMAH, Avignon, France

Abstract—Quantitative ultrasound (QUS) techniques for the estimation of tissue microstructures are based on the frequency analysis of backscattered signals from the tissue. One of these QUS methods relies on theoretical scattering models that match a theoretical backscatter coefficient (BSC) to the measured BSC in order to estimate QUS parameters (such as the effective scatterer size and acoustic concentration). The scattering models generally assume that the tissue under consideration contains identical scatterers in sparse medium and may provide QUS parameters that are not representative of the actual tissue microstructure when the medium is polydisperse in scatterer size and/or dense. Our goal is to study the effects of scatterer polydispersity on QUS estimates by considering three scattering models: the monodisperse sparse model, the polydisperse sparse model and the monodisperse concentrated structure factor model (SFM). In that aim, simulations of backscatter coefficients are conducted with different scatterer size distributions for sparse or moderately dense media. The QUS parameters are estimated at different center frequencies f_0 (from 10 MHz up to 50 MHz) by fitting the simulated backscatter coefficient in the frequency bandwidth $[0.5f_0 - 1.5f_0]$, *i.e.* assuming a transducer with 100% usable bandwidth. The choice of scattering models have a high impact on the QUS parameter estimates as function of frequencies for values of ka less than 1.2.

Index Terms—Backscatter, scattering, microstructure, scatterer size, polydisperse

I. INTRODUCTION

Quantitative ultrasound (QUS) techniques for the estimation of tissue microstructures are based on the frequency analysis of backscattered signals from the tissues. These techniques are used to differentiate between healthy and pathological tissues, to detect cancers or to monitor the response to a treatment. One of these QUS methods relies on theoretical scattering models that match a theoretical backscatter coefficient (BSC) to the measured BSC to estimate QUS parameters, such as the effective scatterer radius a and acoustic concentration n_z (defined as the product of the scatterer number density n and the square of the relative impedance difference between the scatterers and the surrounding medium γ_z). The most frequently used theoretical scattering models are the spherical Gaussian model [1] that describe tissues as a random inhomogeneous continuum with acoustic impedance fluctuations, and the fluid-filled sphere model [2] that consider tissue as an ensemble of discrete spherical scatterers. Both the spherical Gaussian

model and the fluid-filled sphere model assume sparse scattering media. The effective scatterer size corresponds to the correlation length of impedance fluctuations when using the continuous scattering model, or to the characteristic size of scatterers when using the discrete scattering model. However, the estimation of a single-scatterer size may not be representative of the actual tissue microstructure, since tissue exhibit in the major cases different population sizes of scatterers. Lavarello & Oelze [3] studied the scattering of sparse media whose scatterer size distribution follow a continuous probability density function (PDF), and demonstrated that the characteristic size estimates may not match the actual structure sizes. Roberjot et al. [4] and Mamou et al. [5] estimated the characteristic size by using single-scatterer models when the sparse scattering media contains two-population sizes of scatterers. It has been shown that scatterer size estimates vary depending upon the chosen frequency bandwidth [4], and that the smaller scatterers are resolved only when the number density or acoustic impedance contrast of the smaller scatterers is much larger than that of the larger scatterers [5].

Another class of theoretical scattering model is the concentrated Structure Factor Model (SFM), that describes tissue as an ensemble of discrete scatterers and considers interference effects caused by correlations among scatterer positions, which are modeled using a structure factor [6]. The monodisperse concentrated SFM parameterizes the BSC with three indices: the scatterer size, the volume fraction and the impedance acoustic contrast. The concentrated SFM was demonstrated to be the most appropriate model for modeling densely packed cells in *in vitro* cell pellet biophantoms [6]. This modeling was used by Muleki et al. [7] and Muleki & O'Brien [8] to blindly estimate the QUS parameters from a single measured BSC on *ex vivo* tumors. The interpretation of these QUS parameters suggest that the dominant source of scattering could be the whole cells in *ex vivo* HT29 tumors [7], or the nuclei in *ex vivo* tumors of other cell lines (4T1, JC, LMTK and MAT) [8]. However, the polydispersity in scatterer size was shown to affect the BSC behavior in the case of dense scattering media [9]–[12]. An increase in cellular size variance has a significant contribution to the increases in BSC amplitude after cell death in cell pellet biophantoms exposed to chemotherapy [9], [10]. The increase in the size distribution of red blood cell aggregates strongly affect the BSC behavior in flowing blood [11], [12]. So the QUS parameters estimated by the

This work has been carried out thanks to the Excellence Initiative of Aix-Marseille University - A*MIDEX (ANR-11-IDEX-0001), a French Investments d'Avenir programme, in the framework of the Labex MEC.

monodisperse concentrated model may be biased when considering polydisperse scattering media. Franceschini et al. [13] compares monodisperse and polydisperse concentrated SFM to estimate scatterer size and acoustic concentration from cell pellet biophantoms with a range of scatterer volume fractions. They observed similar QUS parameters for both monodisperse and polydisperse concentrated SFM for the studied case of $6.4 \pm 0.9 \mu\text{m}$ cell radii [13]. (Note that in this work [13], the whole cell size variance was assumed to be known *a priori* when using the polydisperse modeling, in order to reduce the number of unknown parameters in the inverse problem.) But wider size distribution needs to be studied to determine the biases on scatterer size estimates when using the monodisperse concentrated SFM.

The aim of this work is to study the effects of scatterer polydispersity on QUS estimates by considering three scattering models: the monodisperse sparse model (fluid-filled sphere model), the polydisperse sparse model and the monodisperse concentrated SFM. To that aim, simulations of BSCs are conducted with different scatterer size distributions (mean radius $a=5.8 \mu\text{m}$ and standard deviations from 0.6 to $2.4 \mu\text{m}$) for sparse or moderately dense media (volume fractions of 1% and 20%). The QUS parameters are estimated by fitting the simulated BSC with one of the three scattering models at different center frequencies f_0 from 10 MHz up to 50 MHz .

II. METHODS

A. Scattering ultrasonic theories

Three discrete scattering theories were considered in this study to estimate the QUS parameters: the monodisperse sparse model (*model 1*), the polydisperse sparse model (*model 2*) and the monodisperse concentrated model (*model 3*). All three models consider a collection of fluid spheres in a surrounding fluid medium. We assumed weak scattering contrast such that the differential backscattering cross section from a single fluid-filled sphere σ_b was calculated as follows:

$$\sigma_b(k, r) = \frac{k^4 V_s^2 \gamma_z^2}{4\pi^2} \left(3 \frac{\sin(2kr) - 2kr \cos(2kr)}{(2kr)^3} \right)^2, \quad (1)$$

where r is the sphere radius, V_s the sphere volume and γ_z the relative impedance contrast.

By considering an ensemble of identical fluid-filled spheres, the theoretical BSC using the monodisperse sparse model (*model 1*) is given by [2]

$$BSC_{sparse}^{monod}(k) = n\sigma_b(k, a), \quad (2)$$

where n is the number density of scatterers. With the model 1, the unknown parameters are the scatterer radius a^* and the acoustic concentration n_z^* .

By considering a mixture of spheres differing only in size, the theoretical BSC using the polydisperse sparse model (*model 2*) can be expressed as:

$$BSC_{sparse}^{polyd}(k) = n \int_0^\infty p(r) \sigma_b(k, r) dr, \quad (3)$$

where $p(r)$ is the sphere radius probability distribution function PDF (*i.e.*, the probability that the sphere radius takes the value r). The number density n is related to the total sphere concentration ϕ as $n = \frac{\phi}{(4/3)\pi \int_0^\infty p(r)r^3 dr}$. The sphere radius distribution is assumed to be gamma distributed, so that the PDF is defined by the mean radius \bar{a} and the gamma width factor ζ (a large value of ζ corresponds to a narrow size distribution). With the model 2, the unknown parameters are the scatterer radius \bar{a}^* , the gamma width factor ζ^* and the acoustic concentration n_z^* .

The models 1 and 2 are only valid if the medium has a low scatterer concentration. At high scatterer concentrations, the interference effects caused by correlations between the spatial positions of individual scatterers can be taken into account by considering the structure factor $S(k)$ [14]. The theoretical BSC using the monodisperse concentrated model (*model 3*) is given by [6], [14]

$$BSC_{dense}^{monod}(k) = n\sigma_b(k, a)S(k, a, \phi). \quad (4)$$

With the model 3, the three unknown parameters are the radius a^* , the volume fraction ϕ^* and the relative acoustic impedance difference γ_z^* .

B. Simulations

Three-dimensional (3D) simulations were performed on an ensemble of spheres uniformly randomly distributed within a simulated volume V_{sim} using a Monte Carlo algorithm [15, section II.B.A]. The simulated volume was fixed to be $400 \times 400 \times 400 \mu\text{m}^3$. Collections of fluid polydisperse spheres were studied to mimic cell biophantoms as done previously in [13]. The sphere size is gamma distributed. The mean radius was equal to $a=5.8 \mu\text{m}$ and the gamma width parameter ζ vary between 5 and 80 (corresponding to standard deviations varying from 0.6 to $2.4 \mu\text{m}$). The relative acoustic impedance difference was chosen to be equal to $\gamma_z=0.11$. Two volume fractions were studied: a low volume fraction $\phi=1\%$ and a moderately dense volume fraction $\phi=20\%$.

The simulated BSC_{sim} was computed as follows:

$$BSC_{sim}(k) = nE \left[\frac{1}{N} \left| \sum_{j=1}^N \Phi(k, a_j) e^{-i2\mathbf{k}\cdot\mathbf{r}_j} \right|^2 \right], \quad (5)$$

where E denotes the ensemble average, r_j is the location of the j th sphere, a_j is the radius of the j th sphere, $\Phi(k, a_j)$ is the scattering amplitude of the j th sphere, N is the total number of spheres that is set by the prescribed volume fraction and n is the sphere number density equal to N/V_{sim} . The BSC_{sim} depends only on the modulus k of the wave vector \mathbf{k} because of the isotropic nature of the studied medium. One simulated BSC_{sim} was computed by averaging over 100 realizations. For each tested volume fraction and each tested standard deviation, this procedure was repeated 10 times to obtain 10 simulated BSC_{sim} .

The simulated BSC was fitted to a theoretical model to estimate QUS parameters. QUS parameters were estimated at

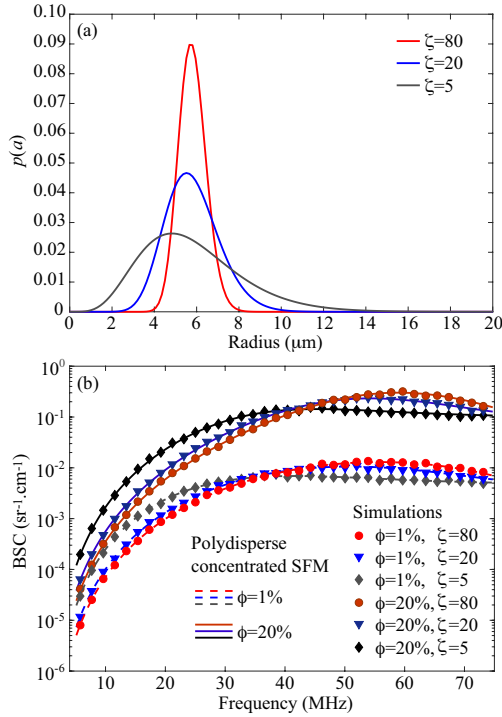


Fig. 1. (a) Scatterer radius PDF with mean radius $a=5.8 \mu\text{m}$ and various gamma width parameters $\zeta=5, 20$ and 80 . (b) Simulated BSC_{sim} (symbols) and theoretical BSC_{theo} computed with the polydisperse concentrated SFM at volume fractions of 1% (dashed lines) and 20% (solid lines).

different center frequencies f_0 by fitting the simulated BSC_{sim} in the frequency bandwidth $[f_{\text{min}} - f_{\text{max}}] = [0.5f_0 - 1.5f_0]$, *i.e.*, assuming a transducer with 100% usable bandwidth.

III. RESULTS AND DISCUSSION

Figure 1 shows the simulated BSC_{sim} in the case of fluid spheres of radius $a=5.8 \mu\text{m}$ with relative acoustic impedance difference $\gamma_z=0.11$ for various gamma width parameters $\zeta=5, 20$ and 80 . Also plotted in Fig. 1 are the theoretical BSC_{theo} computed with the polydisperse concentrated SFM given by Eq. (4) in Ref. [13]. Both simulated BSC_{sim} and theoretical BSC_{theo} are in good agreement. Both changes in scatterer size variance and in volume fractions produce changes in the BSC slope and in the BSC amplitude.

Figure 2 gives the radius a^* and the acoustic concentration n_z^* estimated by the three scattering models when considering an ensemble of fluid spheres sparsely distributed at $\phi=1\%$ and $\zeta=5$ and 80 . The model 1, that does not take into account the polydispersity, estimates correctly the radius and the acoustic concentration for the narrower size distribution with $\zeta=80$. However, when the actual scatterer size variance increases with $\zeta=5$, the model 1 overestimates the scatterer radius and underestimates the acoustic concentration. The scatterer size estimates are larger than the reality because the BSC slope is more influenced by the larger scatterers. Since larger radii have the effect to rise the BSC amplitude, the model 1 underestimates the acoustic concentration to compensate for this effect. The model 2 considering the polydispersity

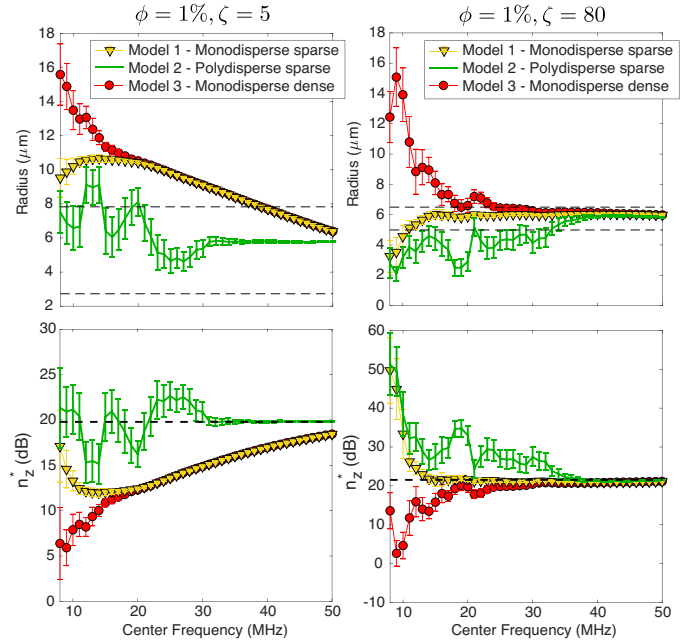


Fig. 2. Scatterer radii a^* and acoustic concentration n_z^* estimated by inversion procedure. Results are obtained from the simulated BSC_{sim} for an ensemble of fluid spheres at $\phi=1\%$, $a=5.8 \mu\text{m}$, $\zeta=5$ and 80 .

shows different results. The mean scatterer radii estimated by the model 2 match very well the actual mean radius for the highly polydisperse medium $\zeta=5$. In the other cases ($\zeta=50, 80$), the model 2 is less efficient than the models 1 and 3 (data not shown for $\zeta=50$). It is interesting to notice that both monodisperse models 1 and 3 gave similar QUS parameters for high frequency values ($f_0 > 20 \text{ MHz}$ $\zeta=5$ and $f_0 > 27 \text{ MHz}$ $\zeta=80$). However, at low frequencies, the model 3 converges more slowly towards actual values when compared to the model 1: scatterer sizes are largely overestimated and acoustic concentrations are underestimated. This is due to the difficulty to estimate simultaneously three parameters a , ϕ and γ_z with the model 3 for diluted media, as discussed previously in [13].

QUS parameters estimated for the moderately dense media $\phi=20\%$ are presented in Fig. 3. Overall, the model 3 provides the best QUS estimates at sufficiently high frequencies ($>30 \text{ MHz}$), and the sparse models 1 and 2 underestimate the mean radius and overestimate the acoustic concentration for the polydispersities $\zeta=20, 50$ and 80 . This limitation is caused by the inability of these sparse models to predict the BSC slope of dense media [13]. For the highly polydisperse medium $\zeta=5$, the scatterer size estimated by the sparse models 1 and 2 fell within the actual size range for a wide range of frequencies. Whatever the considered size variance, there are always some frequencies for which the models 1 and 3 gave similar QUS estimates: 30-50 MHz for $\zeta=5$ and around 50 MHz for $\zeta=20, 50$ and 80 . These results demonstrated that it is not possible to identify a diluted or concentrated medium by comparing the QUS parameters estimated by the sparse and

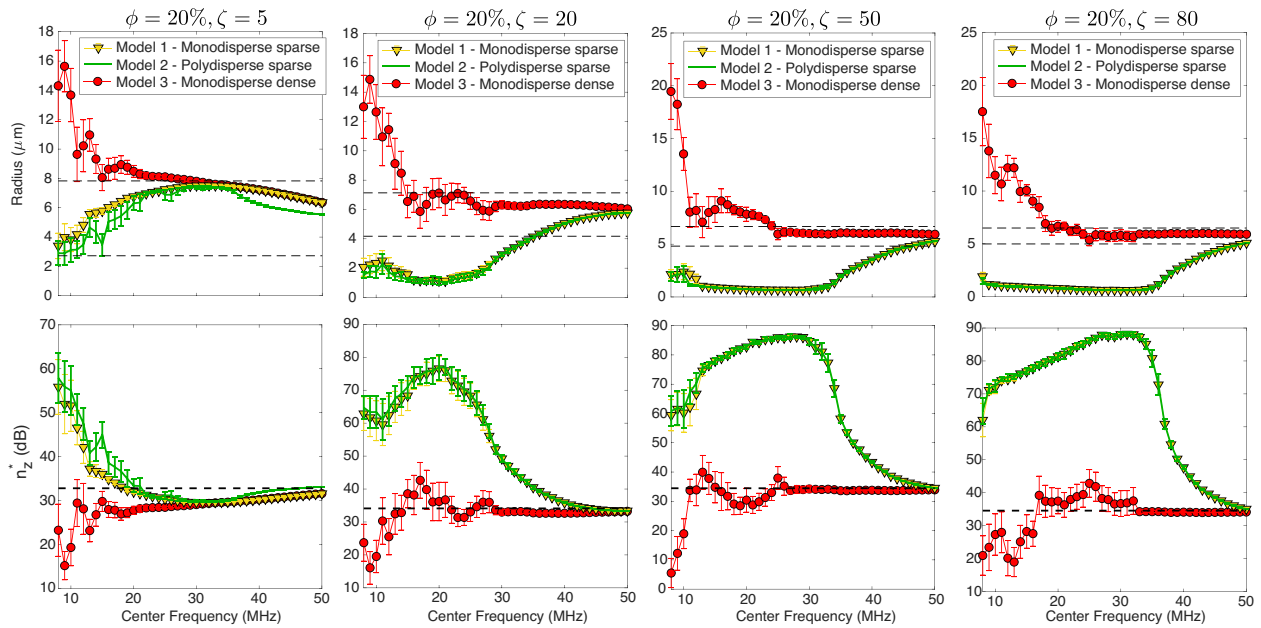


Fig. 3. Scatterer radii \bar{a}^* and acoustic concentration n_z^* estimated by inversion procedure. Results are obtained from the simulated BSC_{sim} for an ensemble of fluid spheres at $\phi=20\%$, $\bar{a}=5.8 \mu\text{m}$, $\zeta=5, 20, 50$ and 80 . In the top panel, the horizontal dashed lines indicate the lower and upper bounds of scatterer radii in the actual radius distribution.

concentrated models, contrary to what we initially suggested in our preliminary study limited to lower frequencies <30 MHz [13].

IV. CONCLUSION

Three models (monodisperse sparse, polydisperse sparse and monodisperse concentrated SFM) were assessed to estimate the scatterer size and acoustic concentration for narrow and wide scatterer size distributions. The results show the limitations of the monodisperse concentrated SFM to estimate scatterer size at low frequencies when considering highly polydisperse scattering media. For the tested scatterer size distributions, the three models converge towards actual values at high frequencies corresponding to product ka around 1.2. Further studies are required to determine the estimate biases when using these models for greater volume fractions ($>20\%$).

REFERENCES

- [1] F. L. Lizzi, M. Greenebaum, E. J. Feleppa, and M. Elbaum, "Theoretical framework for spectrum analysis in ultrasonic tissue characterization", *J. Acoust. Soc. Am.*, vol. 73, no. 4, pp. 1366–1373, 1983.
- [2] M. L. Oelze and W. D. O'Brien, "Application of three scattering models to characterization of solid tumors in mice", *Ultrasonic Imaging*, vol. 28, pp. 83–96, 2006.
- [3] R. Lavarello and M. Oelze, "Quantitative Ultrasound Estimates From Populations of Scatterers With Continuous Size Distribution", *IEEE Trans. Ultras. Ferroelectr. Freq. Control.*, vol. 58, no. 4, pp. 744–753, 2011.
- [4] V. Roberjot, S. L. Bridal, P. Laugier, and G. Berger, "Absolute backscatter coefficient over a wide range of frequencies in a tissue mimicking phantom containing two populations of scatterers", *IEEE Trans. Ultras. Ferroelectr. Freq. Control.*, vol. 43, no. 5, pp. 970–978, 1996.
- [5] J. Mamou, M. L. Oelze, W. D. O'Brien Jr., and J. F. Zachary, "Identifying ultrasonic scattering sites from three-dimensional impedance maps", *J. Acoust. Soc. Am.*, vol. 117, no. 1, pp. 413–423, 2005.
- [6] E. Franceschini, R. Guillermin, F. Tourniaire, S. Roffino, E. Lamy and J.-F. Landrier, "Structure factor model for understanding the measured backscatter coefficients from concentrated cell pellet biophantoms", *J. Acoust. Soc. Am.*, vol. 135, no. 6, pp. 3620–3631, 2014.
- [7] P. Muleki-Seya, R. Guillermin, J. Guglielmi, J. Chen, T. Pourcher, E. Konofagou and E. Franceschini, "High frequency quantitative ultrasound spectroscopy of excised canine livers and mouse tumors using the structure factor model", *IEEE Trans. on Ultrason., Ferroelect., Freq. Contr.*, vol. 63, no. 9, pp. 1335–1350, 2016.
- [8] P. Muleki-Seya and W. O'Brien, "Ultrasound scattering from cell-pellet biophantoms and ex vivo tumors provides insight into the cellular structure involved in scattering", *IEEE Trans. on Ultrason., Ferroelect., Freq. Contr.*, vol. 69, no. 2, pp. 637–649, 2022.
- [9] M. Vlad, R. K. Saha, N. M. Alajez, S. Ranieri, G. J. Czarnota and M. C. Kolios, "An increase in cellular size variance contributes to the increase in ultrasound backscatter during cell death," *Ultrasound Med. Biol.*, vol. 36, no. 9, pp. 1546–1558, 2010.
- [10] E. Franceschini, L. Balasse, S. Roffino and B. Guillet, "Probe the cellular size distribution from cell samples undergoing cell death," *Ultrasound Med. Biol.*, vol. 45, no. 7, pp. 1787–1798, 2019.
- [11] R. de Monchy, J. Rouyer, F. Destrepes, B. Chayer, G. Cloutier and E. Franceschini, "Estimation of polydispersity in aggregating red blood cells by quantitative ultrasound backscatter analysis", *J. Acoust. Soc. Am.*, vol. 143, no. 4, pp. 2207–2216, 2018.
- [12] L. Chinchilla, C. Armstrong, R. Mehri, A. S. Savoia, M. Fenech, E. Franceschini, "Numerical investigations of anisotropic structures of red blood cell aggregates on ultrasonic backscattering", *J. Acoust. Soc. Am.*, vol. 149, no. 4, pp. 2415–2425, 2021.
- [13] E. Franceschini, R. de Monchy and J. Mamou, "Quantitative characterization of tissue microstructure on concentrated cell pellet biophantoms based on the structure factor model", *IEEE Trans. on Ultrason. Ferroelect., Freq. Contr.*, vol. 63, no. 9, pp. 1321–1334, 2016.
- [14] V. Twersky, "Low-frequency scattering by correlated distributions of randomly oriented particules", *J. Acoust. Soc. Am.*, vol. 81, no. 5, pp. 1609–1618, 1987.
- [15] R. K. Saha and G. Cloutier, "Monte Carlo study on ultrasound backscattering by three-dimensional distributions of red blood cells", *Phys. Rev. E*, vol. 78, 061919, pp. 1–9, 2008.